



Yang, Z., Wang, S., Tian, Q., Wang, B., Hethke, M., McNamara, M. E., Benton, M. J., Xu, X., & Jiang, B. (2019). Palaeoenvironmental reconstruction and biostratigraphic analysis of the Jurassic Yanliao Lagerstätte in northeastern China. *Palaeogeography, Palaeoclimatology, Palaeoecology*, 514, 739-753.  
<https://doi.org/10.1016/j.palaeo.2018.09.030>

Peer reviewed version

License (if available):  
CC BY-NC-ND

Link to published version (if available):  
[10.1016/j.palaeo.2018.09.030](https://doi.org/10.1016/j.palaeo.2018.09.030)

[Link to publication record in Explore Bristol Research](#)  
PDF-document

This is the accepted author manuscript (AAM). The final published version (version of record) is available online via Elsevier at <https://doi.org/10.1016/j.palaeo.2018.09.030>. Please refer to any applicable terms of use of the publisher.

## University of Bristol - Explore Bristol Research

### General rights

This document is made available in accordance with publisher policies. Please cite only the published version using the reference above. Full terms of use are available:  
<http://www.bristol.ac.uk/red/research-policy/pure/user-guides/ebr-terms/>

---

**Palaeoenvironmental reconstruction and biostratigraphic analysis of the  
Jurassic Yanliao Lagerstätte in Northeastern China—a case study**

Zixiao Yang<sup>a</sup>, Shengyu Wang<sup>a</sup>, Qingyi Tian<sup>a</sup>, Bo Wang<sup>b</sup>, Manja Hethke<sup>c</sup>, Maria E.

McNamara<sup>d</sup>, Michael J. Benton<sup>e</sup>, Xing Xu<sup>f</sup>, Baoyu Jiang<sup>a,\*</sup>

<sup>a</sup> *Center for Research and Education on Biological Evolution and Environments, School of  
Earth Sciences and Engineering, Nanjing University, Nanjing 210023, China*

<sup>b</sup> *Nanjing Institute of Geology and Palaeontology, Academia Sinica, 210008 Nanjing,  
Jiangsu, China*

<sup>c</sup> *Institut für Geologische Wissenschaften, Fachbereich Geowissenschaften, Freie Universität  
Berlin, Malteserstrasse 74–100, D–12249 Berlin, Germany*

<sup>d</sup> *School of Biological, Earth and Environmental Sciences, University College Cork, Distillery  
Fields, North Mall, Cork T23 TK30, Ireland.*

<sup>e</sup> *School of Earth Sciences, University of Bristol, Bristol BS8 1RJ, UK.*

<sup>f</sup> *Key Laboratory of Vertebrate Evolution and Human Origins, Institute of Vertebrate  
Paleontology and Paleoanthropology, Academia Sinica, Beijing 100044, China*

<sup>\*</sup> *Corresponding author. Email: byjiang@nju.edu.cn*

**ABSTRACT**

The Middle–Late Jurassic Yanliao Lagerstätte contains numerous exceptionally  
preserved fossils of aquatic and land organisms, including salamanders, dinosaurs, pterosaurs  
and mammaliaforms. Despite extensive study of the diversity and evolutionary implications

of the biota, the palaeoenvironmental setting and taphonomy of the fossils remain poorly understood. In this study, we reconstruct both the palaeoenvironment of the Daohugou locality (one of the most famous Yanliao localities), and the biostratinomy of the fossils. We use high-resolution data from field investigation and excavations to document in detail the stratigraphic succession, lithofacies, facies associations, and biostratinomic features of the Lagerstätte. Our results show that frequent volcanic eruptions generated an extensive volcanoclastic apron and lake(s) in this region. The frequent alternation of thin lacustrine deposits and thick volcanoclastic apron deposits reflects either that the studied area was located in the marginal regions of a single lake, where the frequent influx of volcanoclastic apron material caused substantial fluctuations in lake area and thus the frequent lateral alternation of the two facies, or that many comparatively short-lived lakes developed on the volcanoclastic apron. Most terrestrial insects are preserved in the laminated, normally graded siltstone, claystone and tuff that forms many thin intervals with deposits of graded sandstone, siltstone and tuff in between. Within each interval the terrestrial insects occur in many laminae associated with abundant aquatic organisms, but are particularly abundant in some laminae that directly underlie tuff of fallout origin. Most of these terrestrial insects are interpreted to have been killed in the area adjacent to the studied palaeolake(s) during volcanic eruptions. Their carcasses were transported by influxes of fresh volcanoclastic material, primarily meteoric runoff and possibly minor distal pyroclastic flow into the palaeolake(s), where they became buried prior to extended decay probably due to a combination of rapid vertical settling, ash fall and water turbulence.

45 **Keywords:** Palaeoenvironment; Taphonomy; Jurassic; Yanliao Biota; NE China

46

## 1. Introduction

The Middle to Late Jurassic lacustrine deposits in the region encompassing the confluence of Inner Mongolia, Hebei and Liaoning provinces, northeastern China, preserve numerous exceptionally preserved land and aquatic animal fossils (Fig. 1), including various plants (algae, mosses, lycophytes, sphenophytes, ferns, seed ferns, cycadophytes, ginkgophytes and conifers), invertebrates (bivalves, anostracans, spinicaudatans, arachnids and insects) and vertebrates (fish, salamanders, anurans, squamates, pterosaurs, dinosaurs and mammaliaforms) (Huang et al., 2006; Sullivan et al., 2014; Pott and Jiang, 2017), yielding taxa that represent the earliest examples of their respective clades or reveal key evolutionary transitions (e.g. Gao and Shubin, 2003; Ji et al., 2006; Luo et al., 2007; Xu et al., 2009; Lü et al., 2010; Luo et al., 2011; Xu et al., 2011; Huang et al., 2012; Bi et al., 2014; Cai et al., 2014; Xu et al., 2015). These fossils were originally considered to be members of the Early Cretaceous Jehol Biota (Wang et al., 2000; Yuan, 2000), but subsequently proved to be of Middle–Late Jurassic age; they are currently referred to as the Daohugou Biota (e.g. Zhang, 2002) or part of the Yanliao Biota (e.g. Ren et al., 2002; Zhou et al., 2010; Xu et al., 2016). This paper follows the latter terminology, as the extent to which the term “Daohugou Biota” is applicable to the strata containing similar biotas outside the Daohugou region is currently debated (Zhou et al., 2010; Huang, 2016; Xu et al., 2016). The Yanliao Biota spans about 10 million years, and is divided into two phases: the Bathonian–Callovian Daohugou phase and the Oxfordian Linglongta phase, named after representative fossil localities (Xu et al., 2016).

Fossils from the Yanliao biota are often well articulated and exceptionally preserved. Available evidence indicates that many are autochthonous or parautochthonous, or

allochthonous with very limited evidence of decay. Examples include (i) densely packed valves of Spinicaudata (so-called clam shrimps) that preserve delicate carapace ornamentation and sometimes soft-tissue remains such as the head, telson, antennae and eggs (Shen et al., 2003; Liao et al., 2017); (ii) Ginkgoales with leaves attached to shoots and with ovule clusters connected to the peduncle (Zhou et al., 2007); (iii) preservation of fragile structures such as filiform antennae, tarsomeres with spines and hairs and abdominal appendages in cicadas (Wang et al., 2013); (iv) preservation of soft tissue features such as body outlines, gill rakers, external gill filaments, caudal fins, eyes, liver, and even intestinal contents in salamanders (Gao et al., 2013); (v) preservation of exquisite integumentary structures including keratinous ungula sheaths, multi-layered wing membrane structures and densely packed melanosomes in pterosaurs (Kellner et al., 2010; Li et al., 2014); (vi) preservation of filamentous, ribbon-like and pennaceous feathers (and their constituent melanosomes) in dinosaurs (Xu and Zhang, 2005; Zhang et al., 2008; Xu et al., 2009; Xu et al., 2011; Li et al., 2014); and (vi) preservation of hair, patagia, and skin in mammaliaforms despite sometimes only partial preservation of the skeleton (Bi et al., 2014; Ji et al., 2006; Luo et al., 2007; Meng et al., 2006). These fossils have contributed significantly to our understanding of Jurassic terrestrial ecosystems, especially in terms of the evolution of paravians, integumentary structures such as feathers and fur and the ecological diversification of mammaliaforms (Xu et al., 2014; Martin et al., 2015). The biota is rapidly emerging as one of the most important Mesozoic Lagerstätten.

Despite extensive research on the biotic diversity and evolutionary significance of the Yanliao biota, the palaeoenvironmental setting is poorly understood (Wang et al., 2009; Liu et

---

al., 2010; Wang et al., 2013; Na et al., 2015; Huang, 2016; Xu et al., 2016). It is widely accepted that the fossils are hosted within laminated lacustrine deposits. It is unclear, however, whether these deposits represent a single lake or several lakes. The terrestrial members of the biota are considered to have been killed by volcanic activity based on the extensive distribution of volcanic rocks in the Yanliao sequences (e.g. Liu et al., 2010; Yuan et al., 2010; Wang et al., 2013), but the biostratigraphy of the fossils is poorly understood.

In this study, we present the results of a systematic study of the sedimentology and palaeoenvironment of the Middle–Late Jurassic sequence at Daohugou (Fig. 1). Our results reveal key characteristics such as lake origin, depositional model and ecosystem, in addition to potential environmental factors that influenced exceptional fossil preservation.

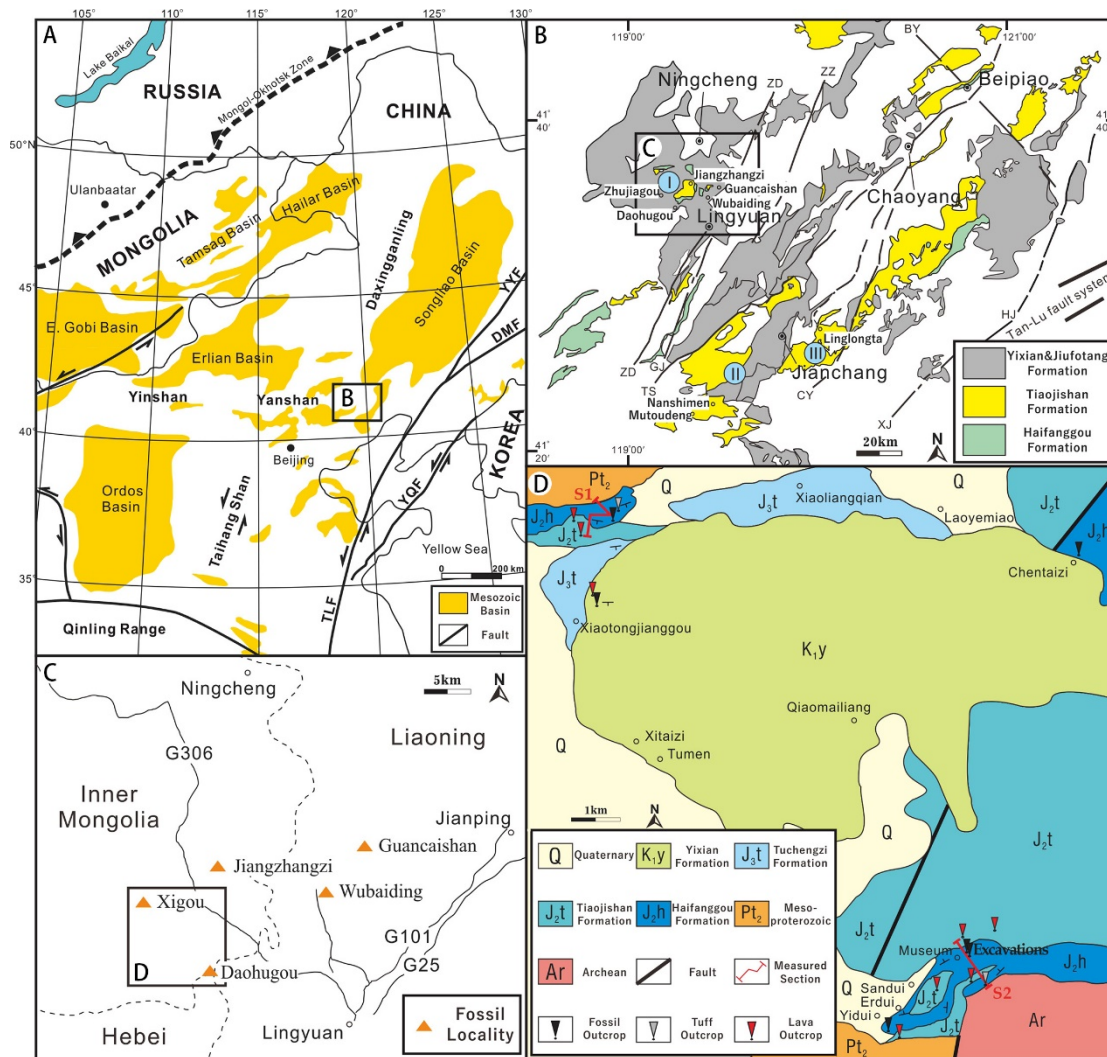


**Fig. 1.** Geological and geographic setting of the studied area. A. Tectonic framework and distribution of the Mesozoic basins in the Yinshan–Yanshan tectonic belt (modified from Meng, 2003 and Y. Zhang et al., 2008); DMF, Dunhua–Mishan fault; TLF, Tan–Lu fault YYF; YQF, Yalvjiang–Qingdao fault; Yilan–Yitong fault. B. Distribution of the Yixian/Jiufotang, Tiaojishan, and Haifanggou formations in a series of northeast-oriented basins (modified from Jiang and Sha, 2006); I, Lingyuan–Sanshijiazi basin; II, Jianchang basin; III, Jinlingsi–Yangshan basin; BY, Beipiao–Yixian fault; CY, Chaoyang–Yaowangmiao fault; GJ, Western Guojiadian Basin fault; HJ, Hartao–Jinzhou fault; TS, Western Tangshenmiao Basin fault; XJ, Xipingpo–Jinxi fault; ZD, Zhangjiayingzi–



Daoerdeng fault; ZZ, Zhuluke–Zhongsanjia fault. C–D. Geographic map of the studied area (C) and geological sketch map (D) show the studied outcrops and sections (modified from Liu et al., 2004).

## 2. Geological Setting

The studied area lies at the easternmost edge of the Yinshan–Yanshan tectonic belt (Davis et al., 1998; Zhang et al., 2008), which extends westward at least 1100 km from China's east coast to Inner Mongolia along the northern edge of the North China craton (Fig. 1A). This belt is interpreted as having formed under the far-field effects of synchronous convergence of two plates (the Siberian in the north and the palaeo-Pacific in the east) toward the East Asian continent, during the Middle Jurassic to Early Cretaceous (Nie et al., 1990; Yin and Nie, 1996; Ziegler et al., 1996; Zhang et al., 2008). Structures in the western and central parts of the belt have predominantly eastward trends, which switch to northeastward trends in the easternmost part. The most obvious fold structures are synclines (and synforms) filled with Jurassic and Cretaceous strata; these are separated from anticlines with Precambrian rocks at the core by thrust and reverse faults that dip away from syncline hinges (Davis et al., 1998). The Yanliao Biota was discovered in the Jurassic Haifanggou and Tiaojishan formations (or Lanqi Formation in studies earlier than the 1990s) in three of these northeast-trending synclines (and synforms), belonging to the following basins: Lingyuan-Sanshijiazhi (localities at Daohugou (including sites at Xigou, Chentaizi and Daohugou village), Zhujiagou and Jiangzhangzi in southeastern Inner Mongolia, and at Wubaiding and Guancaishan in Western Liaoning Province), Jianchang (localities at Mutoudeng (including

Fanzhangzi and Bawanggou), and Nanshimen in northern Hebei Province) and Jinlingsi–  
Yangshan (the Daxishan locality in Linglongta Town, Western Liaoning Province) (Fig. 1B)  
(Wang et al., 1989; Wang et al., 2005; Sullivan et al., 2014; Huang, 2016; Xu et al., 2016).

The Jurassic strata in these basins unconformably overlie the Triassic (or older) strata and  
unconformably underlie the Lower Cretaceous Yixian and Jiufotang formations that yield the  
Jehol Biota (Figs. 1B, 1D and 2A). The Jurassic sequence consists of two stratigraphic  
successions bounded by a regional unconformity. The lower succession comprises the  
volcanic Xinglonggou Formation and the overlying succession, the coal-bearing Beipiao  
Formation. The upper succession is composed of the volcanic Haifanggou and Tiaojishan  
formations and the overlying Tuchengzi Formation (Wang et al., 1989). The geochronological  
framework of the sequence is constrained by radiometric dating, which indicates that the  
Xinglonggou, Tiaojishan and Tuchengzi formations are 177 Ma, 166–153 Ma and 154–137  
Ma, respectively (Yang and Li, 2008; Xu et al., 2012; Xu et al., 2016).

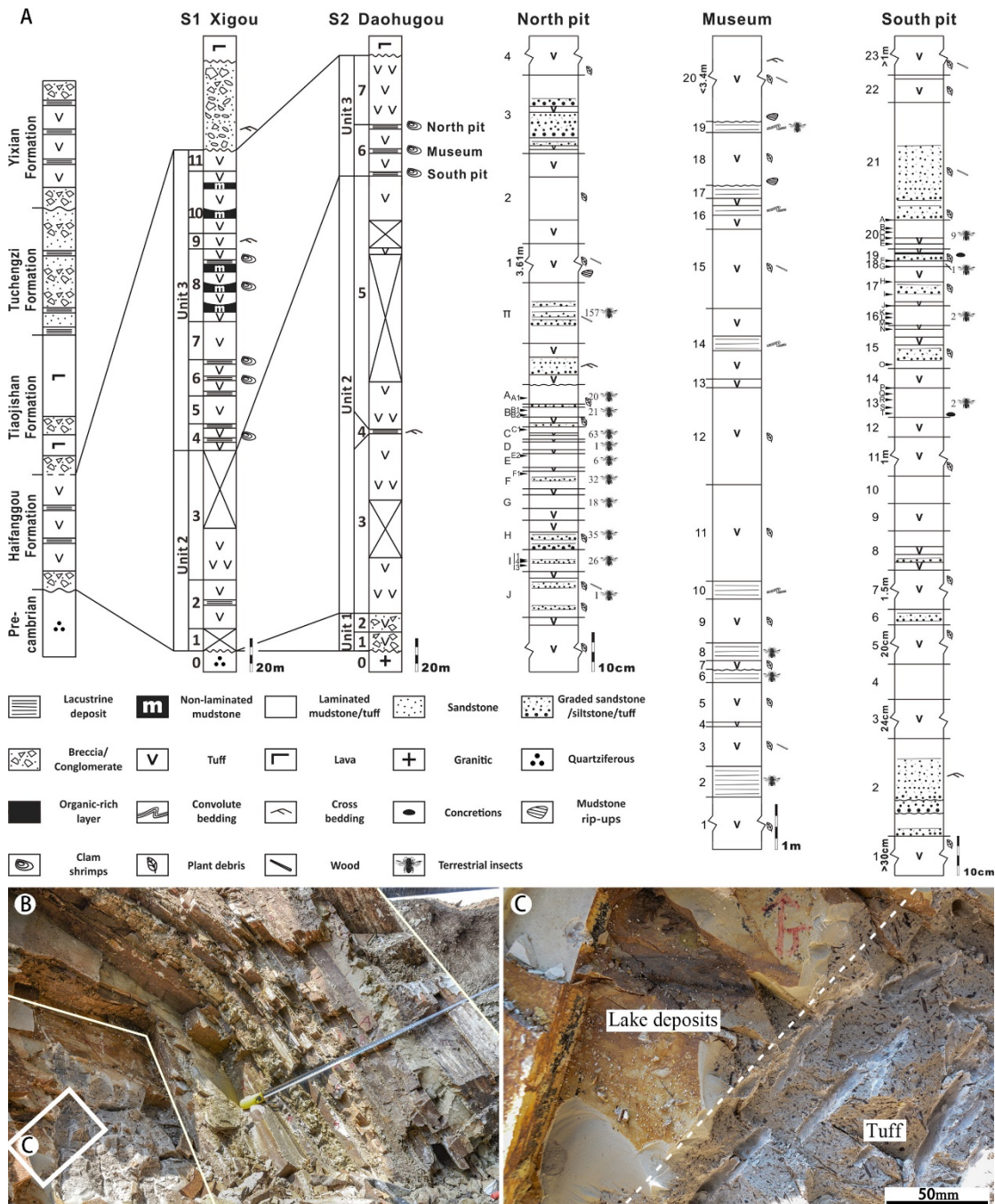


**Fig. 2.** A. Stratigraphy (left) of the Mesozoic and the Haifanggou Formation (S1, S2, locations shown in Fig. 1D) in the Daohugou area, and high-resolution sections (right) from the two excavation pits and the Daohugou Palaeontological Fossil Museum (locations shown in Fig. 1D) showing occurrence horizons and amounts of collected terrestrial insects. B. Excavated section in north pit shows that lacustrine deposits (between the lines) directly overlie and underlie crudely bedded tuffs (bottom is on the lower left). C. Close-up view of

the transition from crudely bedded tuff to laminated lake deposits.

The interval that contains the Yanliao Biota in the Daohugou region, the Daohugou Beds, was assigned to the Haifanggou Formation in an early systematic survey of Mesozoic stratigraphy and palaeontology in western Liaoning (Wang et al., 1989). This was supported by evidence from invertebrate and plant fossils (Zhang, 2002; Shen et al., 2003; Huang et al., 2006; Jiang, 2006). The Haifanggou Formation was considered to be coeval with the Jiulongshan Formation in Beijing and Hebei in many previous studies (e.g. Ren et al., 2002; Shen et al., 2003; Huang et al., 2006; Jiang, 2006). The former differs significantly, however, from the typical Jiulongshan Formation in thickness, associated overlying and underlying strata, and position relative to the regional unconformity, as discussed by Bao et al. (1996) and Li et al. (1996). At a regional scale, the Haifanggou Formation disconformably overlies the Beipiao Formation or older strata, and conformably or disconformably underlies the Tiaojishan Formation. It is composed of polymictic conglomerates intercalated with tuffs, coals and sandstones in the lower part, and interbedded with sandstones, mudstones, and locally rhyolitic lavas in the upper part (Wang et al., 1989; Yang et al., 1997). In the studied area, the Haifanggou Formation unconformably overlies Archean granite gneiss or Mesoproterozoic quartz sandstone and conglomerate, and conformably or locally unconformably underlies volcanic breccia, tuffaceous conglomerate and intermediate or basic lava of the Tiaojishan Formation (Figs. 1D and 2A). The local low-angle unconformity between the Haifanggou and Tiaojishan formations (Huang, 2015) probably resulted from intense volcanic activity. Recent radiometric ages of the volcanic rocks overlying fossil-

bearing strata in the Daohugou region include 165–164 Ma (Chen et al., 2004), 159.8 Ma (He et al., 2004) and 164–158 Ma (Liu et al., 2006), indicating a largely Bathonian to Callovian age for the Haifanggou Formation, corresponding to the older Daohugou phase of the Yanliao Biota (Xu et al., 2016).

### 3. Methods

Two relatively continuous sections were measured (S1 and S2 in Figs. 1D and 2A). Small-scale excavations (about 15–20 m<sup>2</sup> in area and 3–4 m deep; Figs. 1D and 2) were conducted on two fossiliferous intervals to document, at a sub-centimetre scale, the diversity, abundance, completeness and articulation, and plan-view orientation (Supplementary material Appendix 1) of fossils and the lithology of the host strata. A detailed quantitative palaeobiological analysis of the fossil specimens will be presented elsewhere (Wang et al., in prep.). A total of 216 thin sections of representative lithofacies were prepared for petrographic analysis.

### 4. Results

#### *4.1 Stratigraphy*

The two measured sections (S1 and S2 in Fig. 2A) reveal that the Daohugou Beds at the Daohugou locality consist of three units, in ascending order: (1) greenish grey, massive lapilli tuff-breccia with rare grey, laminated mudstone intercalations; (2) greenish to pinkish grey, crudely bedded to massive tuff with rare intercalations of grey, graded sandstone, siltstone and tuff, grey laminated mudstone and grey to white, laminated to thinly bedded tuff; (3)

greenish to pinkish grey, crudely bedded to massive tuff alternating with grey, laminated to horizontally bedded lacustrine deposits, yielding abundant fossils of insects, clam shrimps, plants and rare vertebrates.

Previous research showed that most Yanliao fossils were recovered from the laminated lacustrine deposits of Unit 3 (Sullivan et al., 2014; Cheng et al., 2015; Luo et al., 2015) (Fig. 2A). Poorly preserved fossils of bivalves, anostracans, clam shrimps, insects and plants have also been reported from rare laminated mudstone intercalations in Unit 1 (Huang et al., 2015).

## *4.2 Depositional environments*

### *4.2.1 Petrology*

The classification of the volcanoclastic rocks in this paper follows Schmid (1981). Sediments of the Daohugou Beds are mostly volcanoclastics, consisting mainly of angular crystals of quartz and vitric shards, with minor plagioclase, biotite and pumice, and rare scoria and juvenile lithics in a vitric or argillaceous matrix (Figs. 3 and 4). Vitric grains are usually blocky, platy or moss-like in shape exhibiting low vesicularity, with minor Y-shaped bobble wall shards, and fine- to extremely fine-grained (mostly 20–60  $\mu\text{m}$  wide) (Figs. 3B–C and 4B–D). The dominant angular volcanoclasts and their fine grain size, and morphology of the vitric grains suggest that the eruptions were mainly phreatomagmatic (Heiken, 1972; Self, 1983; Fisher and Schmincke, 2012).





**Fig. 3.** Sedimentary texture and structure of crudely bedded to massive tuff and breccia-



221 bearing lapilli tuff (Lithofacies 1). A. Plant fragments (p) with preferred orientation,  
222 mudstone rip-ups (m), and juvenile lapilli (j); the coin is 19 mm in diameter. B–C. (B) Y-  
223 shaped and (C) blocky, platy vitric shards in a moss-like matrix; note the separated vesicles in  
224 vitric grains (arrows in C); plane-polarized photomicrographs. D. Crudely parallel to cross  
225 bedding (arrow); the pencil is 15 cm long. E–F. Migrated channel-fill bedding (E) and close-  
226 up of the scoured underlying non-laminated mudstone (F, Lithofacies 5); note the rip-ups  
227 (arrow) derived from the red non-laminated mudstone; the coin is 19 mm in diameter. G.  
228 Large-scale slump of lacustrine deposits (dashed line) within the tuff; note the undisturbed  
229 lacustrine deposits underlying the tuff; the round signs are 17 cm in diameter. H. Outsized  
230 accidental boulder of mudstone (dashed line) within lapilli tuff-breccia; the hammer is 28 cm  
231 long.

232



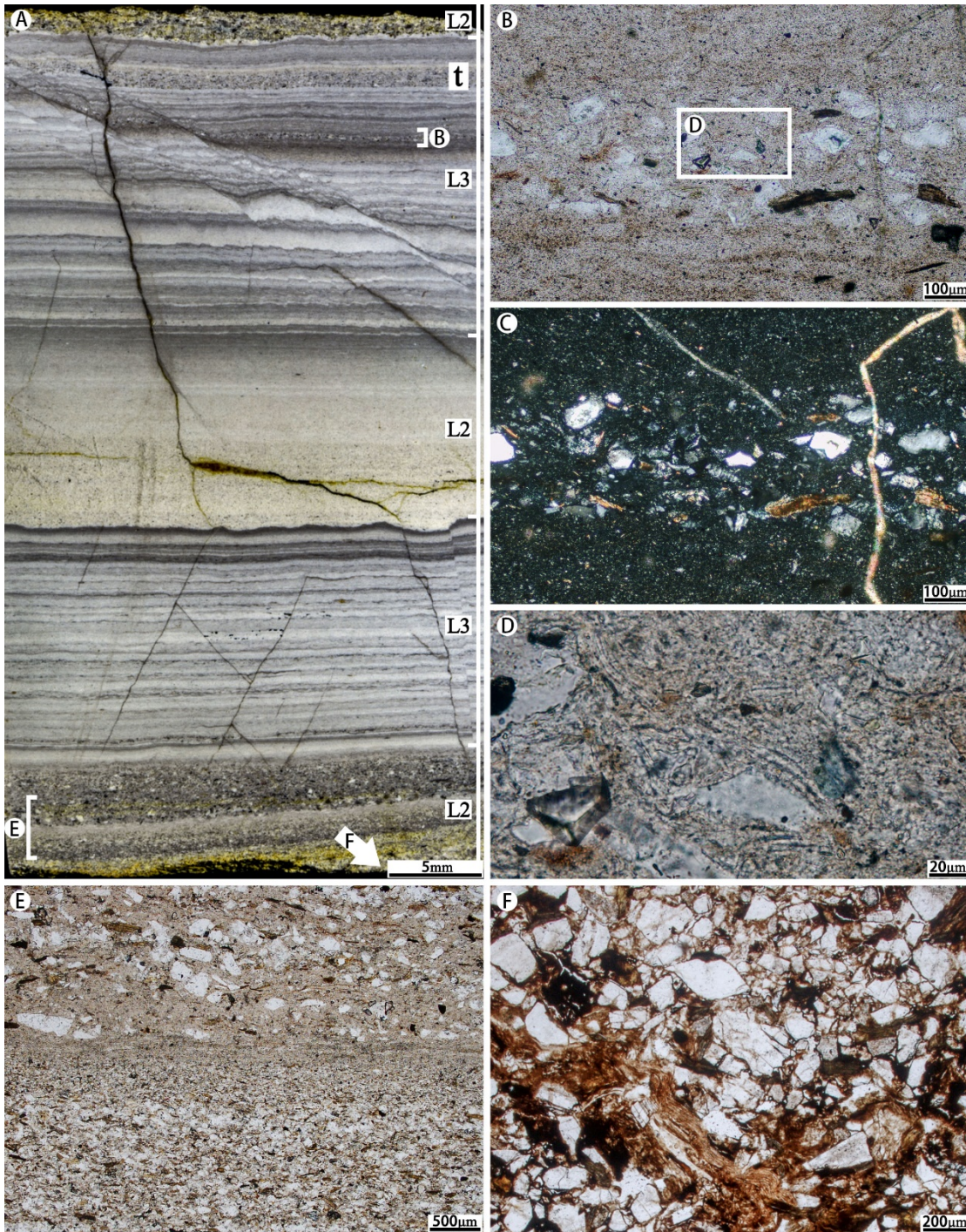


**Fig. 4.** Sedimentary texture and structure of graded sandstone, siltstone and tuff (Lithofacies 2) and laminated, normally graded siltstone, claystone and tuff (Lithofacies 3). A. A polished section from level II (stratigraphic position shown in Fig. 6A) shows alternation of the two lithofacies (L2 and L3) with intercalation of tuff lamina (t, Lithofacies 6). B–C. Close-up view of the thin section marked in A shows the laminated, normally graded siltstone,

claystone and tuff is mainly composed of vitric and crystal grains. D. Close-up view of the rectangle are in B show vitric grains are locally aligned parallel to margins of larger clasts. E–F. Close-up views of the thin section marked in A show normal grading (E) and quenching (F) structures in the graded sandstone, siltstone and tuff. B, D–F, plane-polarized; C, cross-polarized.

The volcanoclastics underwent varying degrees of alteration. Devitrification is particularly common, indicated by fuzzy microcrystalline textures at, and close to, the margins of vitric grains (Figs. 3B–C and 4B–D) (Lofgren, 1971; Streck and Grunder, 1995). X-ray diffraction (XRD) analysis (Supplementary material Appendix 1–2) on the fossil-bearing mudstone from Unit 3 reveals a mean composition including 21.5% montmorillonite and 16.5% illite, reflecting montmorillonitization and subsequent illitization of vitric grains (Fisher and Schmincke, 2012; Huff, 2016), and 22.5% vermiculite, probably weathered from biotite (Pozzuoli et al., 1992).

Pyroclastic flows generated subaerially but deposited subaqueously resemble flows generated by re-sedimentation of fresh volcanic materials in both sediment composition and flow behaviour and thus may produce almost identical deposits, especially for low-temperature and distal pyroclastic flows (Whitham, 1989; Mandeville et al., 1996; Fisher and Schmincke, 2012). The Daohugou volcanoclastics may thus include both pyroclastic and epiclastic deposits, but we categorize these sediments together regardless their origins, in two lithofacies, graded sandstone, siltstone and tuff, and laminated, normally graded siltstone, claystone and tuff, based solely on the common mechanism of sediment transport, i.e.

subaqueous density flow and suspension.

## 4.2.2 Lithofacies

Six lithofacies are recognized here in the Daohugou Beds (Table 1).

Lithofacies	Description	Interpretation	Facies associations*		
			Volcaniclastic apron	Fan delta	Lake floor
1	Crudely bedded to massive tuff and breccia-bearing lapilli tuff	Pyroclastic flow	D	A	
2	Graded sandstone, siltstone and tuff	Transformed subaqueous pyroclastic flow and hyperpycnal flow		D	P
3	Laminated, normally graded siltstone, claystone and tuff	Suspended-load-dominated hyperpycnal flow		A	D
4	Laminated, rhythmic siltstone and claystone	Suspension and distal turbidity current		P	A
5	Non-laminated mudstone	Suspension and distal turbidity current		P	
6	Laminated to thinly bedded tuff	Subaqueous ash fall		A	A

\*D = Dominant; A = Associated; P = Present.

**Table 1** Lithofacies and facies associations of the Daohugou Beds

**Lithofacies 1: Crudely bedded to massive tuff and breccia-bearing lapilli tuff.** This

lithofacies can be massive or crudely bedded, the latter including parallel-, cross-, and channel-fill bedding, and range in thickness from several decimetres to nearly four metres (Fig. 3). The sediments are poorly sorted and occasionally normally graded. Carbonized land plant fragments (up to 0.5 m long) are common (Fig. 3A). Elongated clasts and plant fragments are typically aligned parallel to bedding and often show preferred orientation (Fig. 3A). Vesicles are present as subspherical voids less than 1 mm wide. Irregularly-shaped rip-up clasts of mudstone (cm to dm long) are occasional features at the bases of beds (Fig. 3A, E–F). Accidental lithics (typically 10–30 mm, maximum 2.7 m wide), consist mainly of tuff, granite and mudstone (Fig. 3H) and are rich in lapilli tuff-breccia from Unit 1 (Fig. 2A).

The crude stratification, poor sorting, and preferred orientation of carbonized plant fragments and elongate clasts are characteristic of pyroclastic flow deposits (Buesch, 1992; Branney and Kokelaar, 2002; Fisher and Schmincke, 2012). The carbonized plant fragments were probably engulfed when the flows passed over vegetation, as in modern pyroclastic flows (Hudspeth et al., 2010). The presence of mudstone rip-ups and channel-fill bedding in the basal part of some tuffs indicate the initial flows may have been subaqueous and scoured unconsolidated lacustrine deposits (Whitham, 1989; Mandeville et al., 1996), whereas the absence of evidence for subaqueous transport in the overlying tuffs, such as lamination, sorting, grading, or presence of aquatic fossils, could reflect a shift to subaerial deposition of the subsequent flows. The presence of out-sized boulders of country rocks in Unit 1 suggests the deposits were formed proximal to phreatomagmatic eruptions accompanied by syneruption landslides, lahars or vent-clearing explosions (Belousov and Belousova, 2001; Hungr et al., 2001; Manville et al., 2009).

**Lithofacies 2: Graded sandstone, siltstone and tuff.** This lithofacies consists of

horizontal-, wavy- and cross-stratified, moderately sorted, normally graded sandstone, sandy siltstone and siltstone (Figs. 4A, 4E–F and 6). Strata are usually 0.35–300 mm thick, with a sharp, sometimes erosive base, uneven top and lateral variations in thickness (Figs. 4A and 6). Clasts can exhibit a jigsaw fracture pattern (Fig. 4F). Plant debris is common, as are syndepositional deformational structures, such as load casts, rip-up clasts, convolute bedding and slump structures (Figs. 3G, 4A and 6).

This lithofacies resembles flood deposits generated by hyperpycnal flows (e.g. Kassem and Imran, 2001; Mulder and Alexander, 2001; Alexander and Mulder, 2002; Chapron et al., 2007). The dominant fresh volcanoclastic component of the sediments suggests that the flows represent either influxes of surface runoff carrying recently erupted tephra or distal subaqueous deposits of pyroclastic flows (Whitham, 1989; Mandeville et al., 1996; Mulder and Alexander, 2001; Fisher and Schmincke, 2012). Part of the tephra may have remained sufficiently hot at the site of deposition to produce quenching structures (Whitham, 1989; Büttner et al., 1999; Fisher and Schmincke, 2012).

**Lithofacies 3: Laminated, normally graded siltstone, claystone and tuff.** This

lithofacies occurs mostly in the lower part of Unit 3 (Fig. 2A). It is moderately to well-sorted, and has normally graded laminae with sharp non-erosive bases and uneven tops (Figs. 4A–C and 6). The laminae usually are 100  $\mu\text{m}$ –3 mm thick, but thickness can vary laterally (Fig. 6D). Millimetre-scale soft-sediment deformation structures are common, including wavy lamination and microfaults which locally penetrated and distorted a limited number of laminae (Figs. 4A and 6). Vitric chips locally aligned parallel to the margins of larger clasts



represent possible welding structures (Fig. 4B–D).

The lithofacies bears characteristics of suspended-load-dominated hyperpycnal flow deposits, such as normal grading, sharp but non-erosive base and uneven top, common small-scale syndepositional deformation structures, and closely associated deposits of graded sandstone, siltstone and tuff (Sturm and Matter, 1978; Anderson et al., 1985; Mulder and Chapron, 2011). The flow was very low-energy, unable to erode the lake floor, and deposited sediments from buoyant plumes sympathetic to lake-floor topography (Chapron et al., 2007; Ducassou et al., 2008). The occasional welding structure suggests that part of the tephra may have been remained sufficiently hot at the site of deposition (Whitham, 1989; Fisher and Schmincke, 2012).

**Lithofacies 4: Laminated, rhythmic siltstone and claystone.** This lithofacies is moderately to well-sorted, and consists of laterally persistent couplets of clay-poor (dark) and clay-rich (light) laminae (ca. 30–700  $\mu\text{m}$  thick) with clear bimodal grain size distribution (Fig. 5). Locally the clay-rich laminae exhibit a brown colour (Fig. 5B). This lithofacies occurs as thin intercalations in Lithofacies 3, in particular, at level E from the north pit, and levels 2, 13 and 16 from the south pit.

The lithofacies resulted from predominantly distal turbidity flow and suspension settling (Sturm and Matter, 1978; Anderson et al., 1985; Nelson et al., 1986; Smith, 1986). The couplet laminae probably reflect discontinuous accumulation of the biogenic and fine terrigenous particles, resembling couplets produced in modern seasonally stratified water columns (Sturm and Matter, 1978; Sturm, 1979).

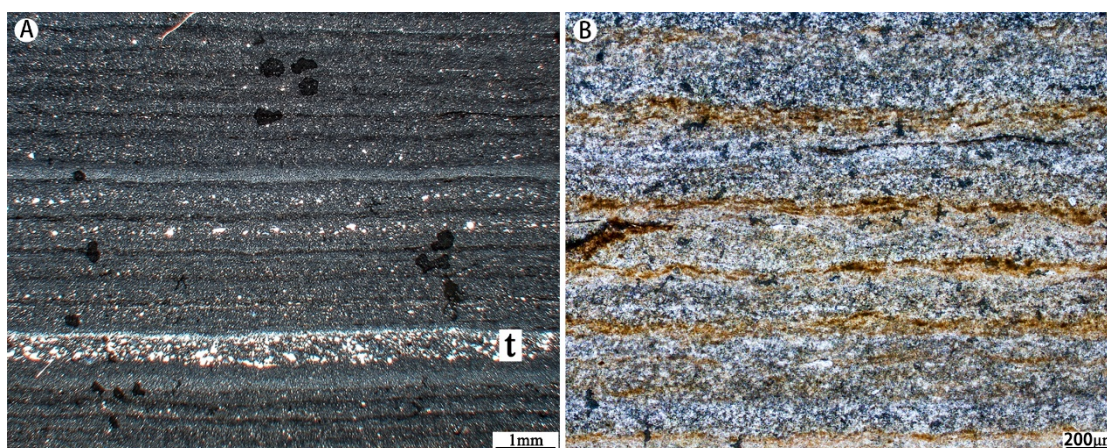


**Fig. 5.** Sedimentary texture and structure of laminated, rhythmic siltstone and claystone. A. Cross-polarized photomicrograph shows regular couplets of clay-rich (dark) and clay-poor (light) laminae interrupted by tuff laminae (t, Lithofacies 6); from a horizon near south pit. B. Plane-polarized photomicrograph shows brown-coloured clay-rich couplet laminae; from level 16 in south pit.

**Lithofacies 5: Non-laminated mudstone.** This lithofacies occurs in the upper part of Unit 3 (Fig. 2A). It occurs as poorly to moderately sorted, normally graded or internally structureless beds 35 mm to ca. 0.8 m thick (Fig. 3E–F).

This lithofacies probably represents distal turbidity flow and suspension deposits (Chun and Chough, 1995; Larsen and Crossey, 1996). The lack of internal structure may reflect extensive bioturbation or rapid deposition of suspended sediment (Sturm, 1979; Reineck and Singh, 2012).

**Lithofacies 6: Laminated to thinly bedded tuff.** This lithofacies occurs as frequent, irregular intercalations of laminae or minor thin beds (200  $\mu\text{m}$ –200 mm thick) in Lithofacies 2–4 (Figs. 5A and 6C). It is laterally persistent with a sharp base and gradual upper contact, fine to extremely fine-grained, and normally graded with a vitric-rich top (Figs. 5A and 6C).

Small plant fragments are common.

This lithofacies is interpreted as subaqueous ash fall deposits based on the dominance of crystal and vitric particles, laterally persistence, associated subaqueous deposits, sharp basal contact and gradual upper contact and normal grading (Niem, 1977; Allen and Cas, 1998; Fisher and Schmincke, 2012).

#### *4.2.3 Facies associations*

The six lithofacies form three facies associations that characterise distinct palaeoenvironments: i.e. volcanoclastic apron, fan delta and lake floor (Table 1).

The volcanoclastic apron comprises Lithofacies 1, i.e., pyroclastic flow deposits associated with proximal fallout and eruption-related lahar deposits (Smith, 1988, 1991; Riggs and Busby-Spera, 1990). The presence of outsized boulders of mudstone in the basal part of the sequence reflects initial vent-clearing explosions that probably occurred when rising magma interacted with water-saturated sediments (Wilson and Walker, 1985; Belousov and Belousova, 2001).

The fan delta is characterized by Lithofacies 2 associated with Lithofacies 1, 3 and 6, with minor Lithofacies 4 and 5. The closely associated deposits of subaerial pyroclastic flow, subaqueous ash fall, hyperpycnal flow and suspension reflect a fan delta environment subject to significant influx of fresh volcanoclastic sediments (Nemec and Steel, 1988; Whitham, 1989; Horton and Schmitt, 1996; Mandeville et al., 1996).

The lake floor comprises mainly Lithofacies 3 associated with Lithofacies 4 and 6, with minor Lithofacies 2. The dominance of distal turbidity current and suspension deposits and



---

abundant aquatic fossils suggest a lake floor environment, typical of the low-energy central basins of temperate lakes (Sturm and Matter, 1978; Nelson et al., 1986; Reineck and Singh, 2012), based on the dominance of sediments formed by hyperpycnal flow. Frequent intercalations of tuff laminae or thin beds indicate that frequent volcanic eruptions occurred in the area.

#### *4.3 Community composition and fossil preservation*

Most fossils are preserved in laminated mudstone (Lithofacies 3 and 4), although rare aquatic fossils, especially clam shrimps, also occur scattered in Lithofacies 2, 5 and 6, and occasionally in Lithofacies 1 (Figs. 2A and 6). With rare exceptions (clam shrimps preserved in three-dimensions in Lithofacies 2 and 5), most fossils are preserved in two dimensions with their ventrodorsal or lateral surface parallel to bedding.

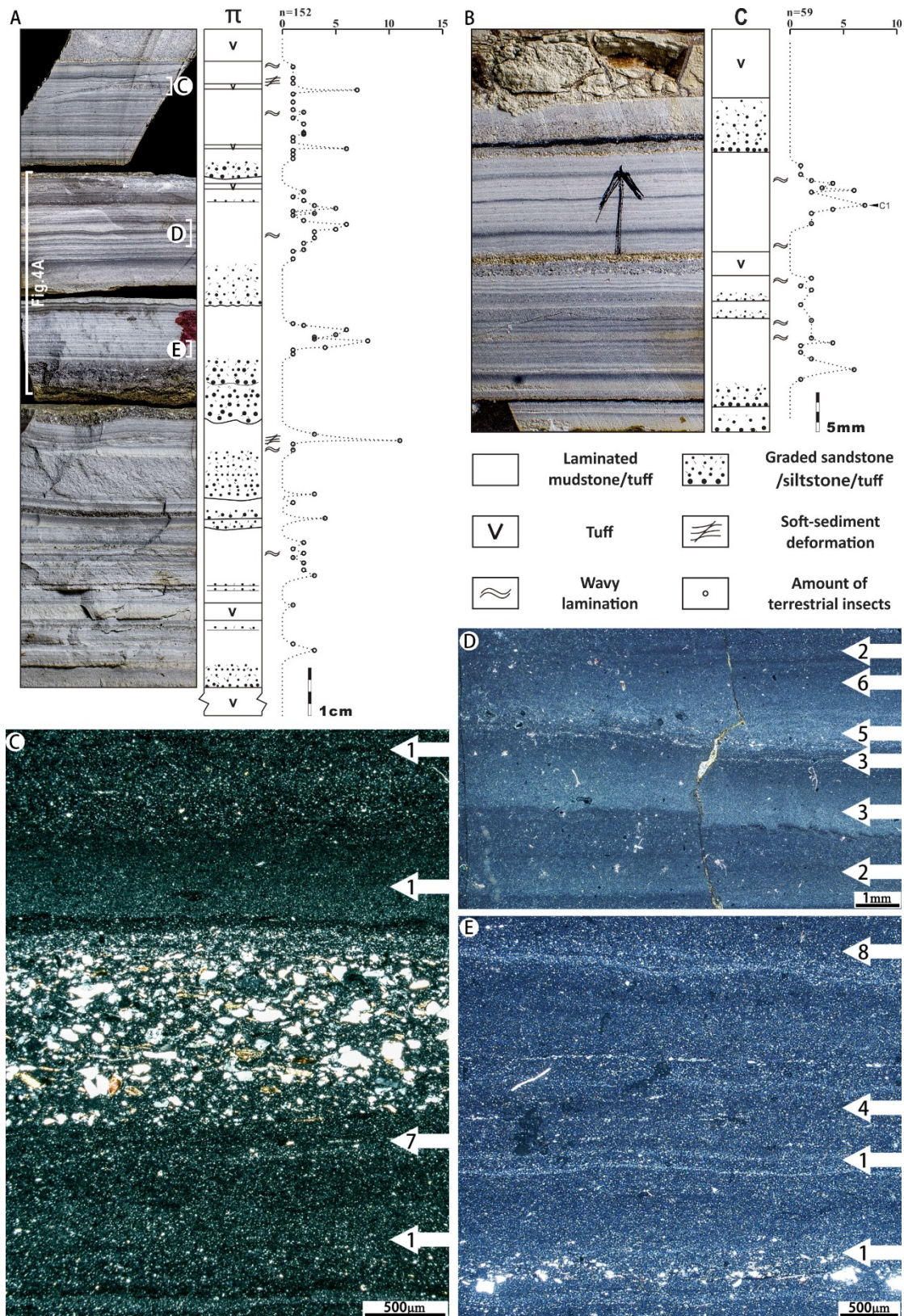


**Fig. 6.** Occurrences and abundance of terrestrial insects. A–B. Polished sections show stratigraphic secessions and number of uncovered terrestrial insects within the fossiliferous

levels II (A) and C (B); 5 and 4 specimens, respectively from II and C levels (see Fig. 2A) were not included due to uncertainty of their exact occurrence horizons. C–E. Cross-polarized photomicrographs of the thin sections from the horizons marked in A show detailed horizons and number of uncovered terrestrial insects.

Benthic aquatic organisms are abundant, but of low diversity. Only four species were identified (Wang et al., in prep.): the clam shrimp *Triglypta haifanggouensis*, recently reviewed by Liao et al. (2017), larvae of the mayfly *Fuyous gregarious* and *Shantous lacustris*, and the water boatman *Daohugocorixa vulcanica*. Clam shrimps are the dominant group of benthic aquatics and occur in all fossiliferous horizons with a density of up to 14487/m<sup>2</sup> (extrapolated from measurement of an 81.45 cm<sup>2</sup> surface). Mayfly larvae and water boatmen are less common. In the 35 quantitatively studied horizons, mayfly larvae occur in 25 horizons with a density of up to 421/m<sup>2</sup> (extrapolated from measurement of a 284.74 cm<sup>2</sup> surface) and water boatmen exist in 21 horizons with a density of up to 251/m<sup>2</sup> (extrapolated from measurement of a 636.9 cm<sup>2</sup> surface) (Wang et al., in prep.). Most aquatic fossils are articulated with little fragmentation and typically retain delicate details such as carapace ornamentation (clam shrimps), tergite and cerci (mayfly larvae), and setae (water boatmen).

Terrestrial animals are represented exclusively by insects and are rare in the south pit (only 14 specimens were recovered in four horizons; Fig. 2A). In contrast, insects are abundant in the north pit, in which 380 specimens representing 15 orders and 57 families were collected from 11 levels (Fig. 2A). Among these, 54.9% of specimens are edaphic taxa, 37.3% sylvan, and 7.8% alpine (Wang et al., in prep.). Most terrestrial insects are preserved in

Lithofacies 3 that forms many thin intervals (ca. 7–28 mm thick) with deposits of lithofacies 2 in between (Figs. 2, 4 and 6). Within each interval the insects occur in many laminae associated with abundant aquatic organisms, but are particularly abundant in some laminae that directly underlie tuff of fallout origin (Fig. 6). The associated aquatic fossils sometimes show preferred plan-view orientation (e.g. horizons B2, C1, F1 and I3, Supplementary material Appendix 2). Most terrestrial insects are well preserved: over 50% of the specimens are complete and articulated, and various fine anatomical details are preserved (e.g., cerci, filiform antennae, tiny spines and setae) (Wang et al., in prep.).

Similarly, terrestrial plants are rare in the south pit (only five specimens were found) but more abundant in the north pit (114 specimens were recovered from the 11 fossiliferous levels mentioned above (Fig. 2A)). The plants include ferns, caytonialeans, bennettites, ginkgophytes, czekanowskialeans and conifers. Among these, tall-growing gymnosperms are dominant, preserving entire or large fragments of leaves and organs, while water- or moisture-bound groups such as ferns are represented by only rare fragmentary remains (Pott and Jiang, 2017).

## 5. Discussion

### 5.1 Depositional model

In the studied area, the lake floor and fan delta deposits are very thin, ranging from ca. 0.2 to 1 m thick, while the volcanoclastic apron deposits, which sandwiched successive lacustrine intervals, are often much thicker (up to at least 4.4 m thick) (Fig. 2A; e.g. levels 11–13 in Museum section). This distribution of lacustrine and volcanoclastic apron deposits



indicates that the lacustrine sediments formed on, and were derived mainly from, volcaniclastic apron deposits that directly underlie and overlie them (Figs. 2 and 7).

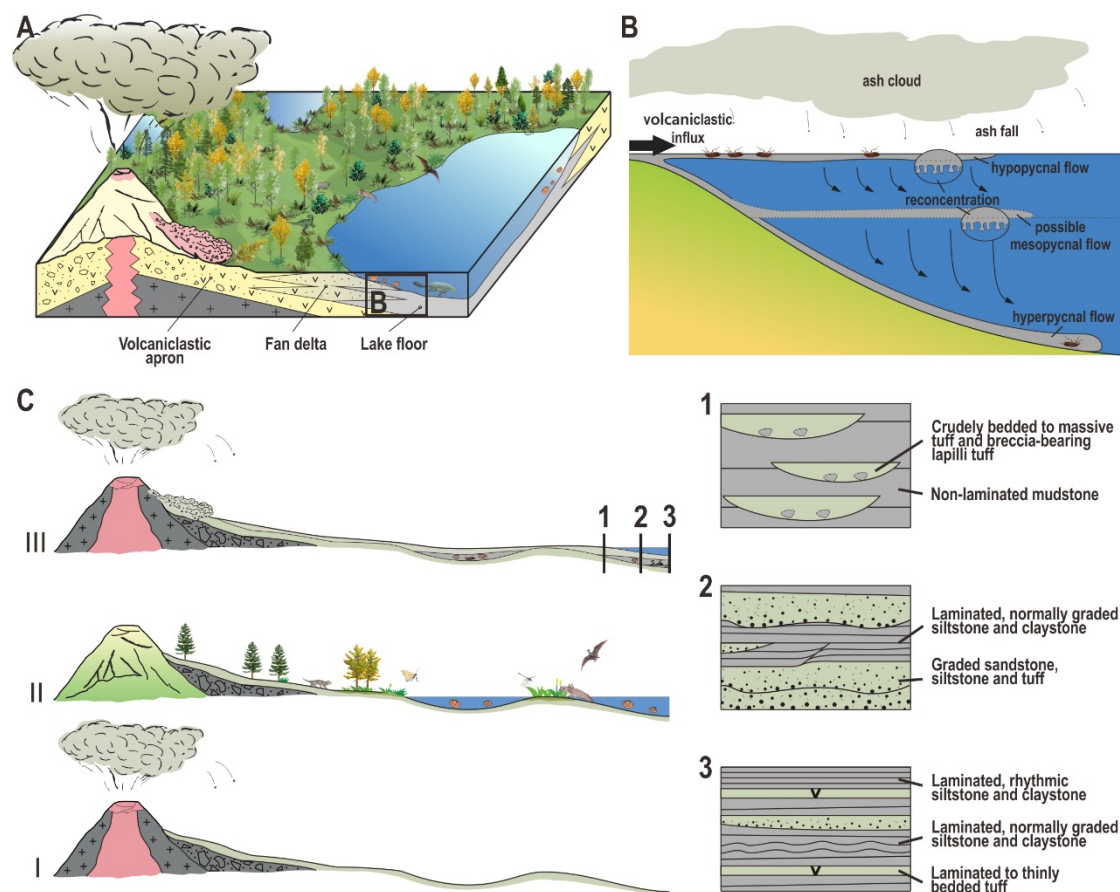


**Fig. 7.** A–B. Depositional model of the Daohugou beds in the studied area (A), and biostratinomic model of the land remains (B). C. Illustrative sketch (not for scale) of the evolution of the Daohugou lake(s): I–II, waterbodies gradually accumulated on the volcaniclastic apron, where the Daohugou ecosystem was established and developed; II–III, during syneruption periods, volcaniclastic influxes repeatedly devastated the ecosystem and buried the remains, and may even have destroyed the lake completely; keys as in Figs. 2 and 3. Some of the animal figures were revised from reconstructions by Rongshan Li, Nobu Tamura and April M. Isch.

There are two scenarios that could account for this frequent alternation of thin lacustrine deposits and thick volcanoclastic apron deposits. The studied section could represent deposition in marginal regions of a single lake, where the frequent influxes of volcanoclastic apron material caused substantial fluctuations in lake area and resulted in the frequent and abrupt lateral alternation of the two facies. The lake must have been bounded by steep margins with restricted development of marginal facies in littoral and shallow-water zones, at least at the studied sites, because there is no evidence for typical shallow-water wave activity such as wave-formed ripples or cross-stratification. Meanwhile the volcanoclastic influxes, including remobilized sediments on the marginal slope, may have frequently disturbed the underlying lacustrine deposits and formed the large mudstone rip-ups and slump structure (Figs. 3A, 3E–G and 6).

Alternatively, many comparatively short-lived lakes could have developed on the volcanoclastic apron in the studied area, as commonly seen in modern analogues (Anderson et al., 1985; Blair, 1987a; Manville et al., 2001; Dale et al., 2005; Christenson et al., 2015). These lakes may have been filled up or breached, and then covered by volcanoclastic apron sediments arising from subsequent eruptions. The extensively disturbed lacustrine deposits (Figs. 3A, 3E–G and 6), thus may reflect the process of filling up or breaching of the lakes, similar to the final lake-fill sequence in the Eocene Challis volcanic field, where extensive pyroclastic deposits filled a ca. 20 m deep intermontane lake (Palmer and Shawkey, 1997, 2001). The fine-textured tephra from the top of the volcanoclastic apron deposits formed a water-tight surface crust after wetting (Dale et al., 2005), upon which another cycle of lake

sediments accumulated (Fig. 7C).

It remains unclear which scenario applies here given the uncertainty about the basin structure and lake topography. Nonetheless, in either case, the hydrological regime clearly changed frequently and rapidly at the studied sites, causing the repeated and abrupt shift from volcanoclastic apron deposits to lacustrine deposits. This may be ascribed to damming of the drainage network by the emplacement of volcanic materials, as their modern and recent counterparts (Scott et al., 1996; Simon, 1999; Palmer and Shawkey, 1997, 2001). Active earthquakes and fault movements in Daohugou area associated with volcanism or tectonics (Liu et al., 2004; Zhang et al., 2008; Huang, 2015) may also have created areas of low topography, disrupting groundwater and surface-water systems (Blair, 1987b; Palmer and Shawkey, 1997, 2001).

## 5.2 Biostratigraphic model

The high abundance of aquatic taxa in the lacustrine deposits reflects a combination of high population densities and background accumulation of aquatic animals (time averaging), especially those embedded in the laminated, rhythmic siltstone and claystone (Lithofacies 4). In contrast, repeated association of high concentrations of terrestrial insects of different niches and various ontogenetic stages (Liu et al., 2010), suggests repeated mass mortality events in the region. The dominant fresh volcanoclastic component of the host sediments and very limited decay of the carcasses before burial (Martínez-Delclòs and Martínell, 1993; Duncan et al., 2003; Wang et al., 2013) suggest that the mass mortality events occurred during, and were probably associated with volcanic eruptions, such as those resulting from modern

eruptions (Baxter, 1990; Dale et al., 2005; Christenson et al., 2015).

The close association of the land animal fossil-bearing laminae (Lithofacies 3) with graded sandstone, siltstone and tuff (Lithofacies 2), indicates that these land animal remains were probably transported into the studied lake(s) by influxes of fresh volcanoclastic material. Transport of terrestrial vertebrates with complete skeletons and extensive soft tissue preservation into lacustrine environments has been linked to high-temperature pyroclastic flow (Jiang et al., 2014). Evidence for hot emplacement in Lithofacies 2 and 3, however, is scarce, suggesting mainly runoff during high discharge periods associated with eruptions and possibly minor distal low-temperature pyroclastic flows (Sigurdsson et al., 1982); such flows carried newly erupted tephra and triggered subaqueous density flows. Organisms in littoral habitats may have been incorporated into the lake(s) *postmortem*.

As commonly observed in many taphonomic experiments, most freshly killed insects remain floating on the water surface in a still water body until significant decay occurs (e.g. Martínez-Delclòs and Martinell, 1993; Duncan et al., 2003; Wang et al., 2013). Indeed, the Daohugou fossils probably drifted far offshore (Fig. 7B), as indicated by the accompanying plant fossil assemblage including mostly large land plants with minor low-growing water-related plants (Pott and Jiang, 2017). The abundance and high fidelity of preservation of insects, however, probably reflects minimal floatation prior to burial. Such rapid sinking may be attributed to turbulent water caused by wind or continuing subaqueous density flow (Martínez-Delclòs and Martinell, 1993), but this conflicts with our evidence that the laminae hosting terrestrial insect fossils (Lithofacies 3) mostly resulted from very low-energy flows dominated by suspension processes. Rather, these thin fossiliferous intervals may reflect



repeated processes of rapid settling of fine-grained sediment particles and the floating remains, by convective sedimentation. In other words, successive reconcentrations of overflow or concentrations of ash fall in the surface water triggered fast-descending convective plumes, forming vertical gravity currents that wrapped the remains, and eventually reached the lake floor and generated the very low-energy hyperpycnal flows (Sturm and Matter, 1978; Carey, 1997; Parsons et al., 2001; Ducassou et al., 2008; Davarpanah and Wells, 2016) (Fig. 7B). This process may result in sedimentation rates one to three orders of magnitude greater than the Stokes settling velocity (Carey, 1997; Davarpanah and Wells, 2016), and thus probably timely sealed the remains and protected them from further decay.

In addition, the particularly fossiliferous laminae directly underlying tuff laminae (Fig. 6A and C) may indicate that, although ash fall may not be concentrated enough to trigger convective sedimentation, it could also cause rapid sinking and burial by simply adding weight to the remains (Tian et al., in prep.).

### *5.3 Palaeoenvironmental implications*

The stratigraphic succession shows that intense volcanic eruptions produced extensive volcanoclastic apron deposits in the studied area. Lake(s) developed on the volcanoclastic apron and were subject to frequent influxes of voluminous volcanoclastic sediments (Fig. 7). The aquatic ecosystem of the lake(s) resembled that of modern short-lived waterbodies, including a low-diversity aquatic fauna and high density of monospecific assemblages, dominated by crustaceans and pond-type salamanders (Vannier et al., 2003; Liu et al., 2010; Sullivan et al., 2014). In particular, clam shrimps yield dormant eggs that may rapidly hatch

after several years (to decades) of drought (Dumont and Negrea, 2002) or without prior desiccation (Bishop, 1967; Hethke et al., submitted). Hence, they disperse through water-, animal- and wind transportation (Tasch, 1969; Webb, 1979; Frank, 1988), and might have easily endured frequent collapses of the lacustrine ecosystem caused by volcanic eruptions. Their successful dispersal strategies mean that clam shrimps would have been able to rapidly colonize newly-built aquatic niches. Ephemerid nymphs and water boatmen were less abundant, and they probably colonized the new post-eruption lake habitats by migrating from nearby aquatic habitats (Batzer and Wissinger, 1996). However the longevity of the lake(s) remains uncertain as ecological comparison between these benthic aquatic taxa of the Haifanggou Formation and their modern relatives is inconclusive. Although clam shrimp population palaeoecology has often been interpreted based on an analogy with extant “shallow and temporary” habitats (e.g., Webb, 1979; Frank, 1988; Vannier et al., 2003; Olempska, 2004), their Mesozoic analogues clearly occupied a much wider ecological space (Olsen, 2016; Hethke et al., submitted). In addition, modern Corixidae can be early colonizers of temporary waters, but many species frequently appear in permanent ponds and lakes as well as streams (e.g. Brown, 1951; Jansson and Reavell, 1999). Further, mayfly nymphs occur in all sorts of water bodies, including shallow areas of deep permanent lakes (e.g. Lyman, 1943; Brittain and Sartori, 2009). The consistently low-diversity associations of clam shrimps, water boatmen and mayfly larvae might thus indicate small regional species richness and high disturbance in connected habitats (Chase, 2003); alternatively, they may reflect a lack of hydrological connectivity.

The presence of highlands surrounding the lake(s) is supported by extensive fan-delta

deposits and the preservation of alpine insects and upland plants in the lacustrine deposits (Liu et al., 2010; Na et al., 2015; Na et al., 2017; Pott and Jiang, 2017). The relatively high abundance of land plant debris in pyroclastic flow deposits and the paucity of epiclasts derived from weathering suggest that the region adjacent to the lake(s) was well vegetated. This is consistent with the inferred warm and humid climate reflected by the Yanliao flora (Liu et al., 2010; Na et al., 2015; Na et al., 2017; Pott and Jiang, 2017).

## 6. Conclusions

Six lithofacies are recognized in the Daohugou Beds, which form three facies associations in space and time, i.e. volcanoclastic apron, fan delta and lake floor. The stratigraphic succession shows that intense volcanic eruptions resulted in an extensive volcanoclastic apron and lake(s) in the studied area. Thin lacustrine deposits frequently alternated with thick volcanoclastic apron deposits. This reflects either that the studied area was located in marginal regions of a single lake, where the frequent influx of volcanoclastic apron material caused substantial fluctuations in lake area and thus the frequent lateral alternation of the two facies, or that many comparatively short-lived lakes developed on the volcanoclastic apron. Most terrestrial insects are preserved in the laminated, normally graded siltstone, claystone and tuff that forms many thin intervals with deposits of graded sandstone, siltstone and tuff in between. Within each interval the terrestrial insects occur in many laminae associated with abundant aquatic organisms, but are particularly abundant in some laminae that directly underlie tuff of fallout origin. Most of these terrestrial insects are interpreted to have been killed during volcanic eruptions. Their carcasses were dropped or

transported by influxes of fresh volcanoclastic material, mostly runoff and possibly minor distal pyroclastic flow into the studied lake(s), where they became rapidly buried prior to extended decay probably due to a combination of rapid vertical settling, ash fall and water turbulence.

## Acknowledgements

The authors thank Qi Zhang, He Wang, Miao Ge, and personnel of the Daohugou National Geopark for their kind support in the field. We are also deeply grateful to Dr. Christian Pott for identifying the plant fossils we collected, to Prof. Franz T. Fürsich, Prof. Frank Riedel and Prof. Volker Lorenz for constructive discussion and suggestions, and to Yingying Zhao for her great help with the drawings. This research was financially supported by the National Science Foundation of China (41672010; 41688103; 41572010) and by a European Research Council Starting Grant H2020–2014–ERC–StG–637698–ANICOLEVO awarded to MMN.

## Data availability

Supplementary materials to this article can be found in the online version of the paper.

## References

- Alexander, J., Mulder, T., 2002. Experimental quasi–steady density currents. *Mar. Geol.* 186, 195–210.
- Allen, S., Cas, R., 1998. Rhyolitic fallout and pyroclastic density current deposits from a

- 
- 601 phreatoplinian eruption in the eastern Aegean Sea, Greece. *J. Volcanol. Geotherm. Res.* 86,  
602 219–251.
- 603 Anderson, R.Y., Dean, W.E., 1988. Lacustrine varve formation through time. *Palaeogeogr.*  
604 *Palaeoclimatol. Palaeoecol.* 62, 215–235.
- 605 Anderson, R.Y., Nuhfer, E.B., Dean, W.E., 1985. Sedimentation in a blast-zone lake at Mount  
606 St. Helens, Washington—implications for varve formation. *Geology* 13, 348–352.
- 607 Büttner, R., Dellino, P., Zimanowski, B., 1999. Identifying magma-water interaction from the  
608 surface features of ash particles. *Nature* 401, 688–690.
- 609 Bao, Y., Liu, Z., Wang, S., 1996. Stratigraphy (lithostratic) of the Municipality of Beijing.  
610 Wuhan: China University of Geosciences Press.
- 611 Batzer, D.P., Wissinger, S.A., 1996. Ecology of insect communities in nontidal wetlands.  
612 *Annu. Rev. Entomol.* 41, 75–100.
- 613 Baxter, P.J., 1990. Medical effects of volcanic eruptions. *Bull. Volcanol.* 52, 532–544.
- 614 Belousov, A., Belousova, M., 2001. Eruptive process, effects and deposits of the 1996 and the  
615 ancient basaltic phreatomagmatic eruptions in Karymskoye lake, Kamchatka, Russia.  
616 Volcanogenic sedimentation in lacustrine settings. *Inte. Ass. Sedimentol. Spec. Publ.* 30,  
617 35–60.
- 618 Bi, S., Wang, Y., Guan, J., Sheng, X., Meng, J., 2014. Three new Jurassic euharamiyidan  
619 species reinforce early divergence of mammals. *Nature* 514, 579–584.
- 620 Bishop, J. A. 1967. Some adaptations of *Limnadia stanleyana* King (Crustacea:  
621 Branchiopoda: Conchostraca) to a temporary freshwater environment. *Journal of Animal*  
622 *Ecology*, 36, 599–609.

- 623 Blair, T.C., 1987a. Sedimentary processes, vertical stratification sequences, and  
624 geomorphology of the Roaring River alluvial fan, Rocky Mountain National Park,  
625 Colorado. *J. Sediment. Res.* 57, 1–18.
- 626 Blair, T.C., 1987b. Tectonic and hydrologic controls on cyclic alluvial fan, fluvial, and  
627 lacustrine rift–basin sedimentation, Jurassic–Lowermost Cretaceous Todos Santos  
628 Formation, Chiapas, Mexico. *J. Sediment. Res.*, 57, 845–862.
- 629 Branney, M.J., Kokelaar, B.P., 2002. Pyroclastic density currents and the sedimentation of  
630 ignimbrites. *Geol. Soc. Lond. Mem.* 27, 1–143.
- 631 Brittain, J. E., & Sartori, M., 2009. Ephemeroptera (Mayflies). In *Encyclopedia of Insects*  
632 (Second Edition), pp. 328–334.
- 633 Brown, E. S., 1951. The relation between migration-rate and type of habitat in aquatic insects,  
634 with special reference to certain species of Corixidae. *Journal of Zoology*, 121, 539–545.
- 635 Buesch, D.C., 1992. Incorporation and redistribution of locally derived lithic fragments within  
636 a pyroclastic flow. *Geol. Soc. Am. Bull.* 104, 1193–1207.
- 637 Cai, C.-Y., Thayer, M.K., Engel, M.S., Newton, A.F., Ortega-Blanco, J., Wang, B., Wang,  
638 X.-D., Huang, D.-Y., 2014. Early origin of parental care in Mesozoic carrion beetles. *Proc.*  
639 *Natl. Acad. Sci., U.S.A.* 111, 14170–14174.
- 640 Carey, S., 1997. Influence of convective sedimentation on the formation of widespread tephra  
641 fall layers in the deep sea. *Geology*, 25, 839–842.
- 642 Chapron, E., Juvigné, E., Mulsow, S., Ariztegui, D., Magand, O., Bertrand, S., Pino, M.,  
643 Chapron, O., 2007. Recent clastic sedimentation processes in Lake Puyehue (Chilean Lake  
644 District, 40.5 S). *Sediment. Geol.* 201, 365–385.

- 645 Chase, J. M., 2003. Community assembly: when should history matter? *Oecologia*, 136, 489–  
646 498.
- 647 Chen, W., Ji, Q., Liu, D. Y., Zhang, Y., Song, B., & Liu, X. Y., 2004. Isotope geochronology  
648 of the fossil-bearing beds in the Daohugou area, Ningcheng, Inner Mongolia. *Regional*  
649 *Geol. China*, 23, 1165–1169.
- 650 Cheng, X., Wang, X., Jiang, S., Kellner, A.W., 2015. Short note on a non-pterosactyloid  
651 pterosaur from Upper Jurassic deposits of Inner Mongolia, China. *Hist. Biol.* 27, 749–754.
- 652 Christenson, B., Németh, K., Rouwet, D., Tassi, F., Vandemeulebrouck, J., Varekamp, J.C.,  
653 2015. *Volcanic Lakes*. Springer, Berlin, Heidelberg.
- 654 Chun, S., Chough, S.K., 1995. The Cretaceous Uhangri formation, SW Korea: lacustrine  
655 margin facies. *Sedimentology* 42, 293–322.
- 656 Dale, V.H., Swanson, F.J., Crisafulli, C.M., 2005. Disturbance, survival, and succession:  
657 understanding ecological responses to the 1980 eruption of Mount St. Helens. In: Dale VH,  
658 Swanson FJ, Crisafulli C.M. (Eds.), *Ecological responses to the 1980 eruption of Mount*  
659 *St. Helens*. New York, NY: Springer; 2005. pp. 3–11.
- 660 Davarpanah Jazi, S., Wells, M. G., 2016. Enhanced sedimentation beneath particle-laden  
661 flows in lakes and the ocean due to double-diffusive convection. *Geophysical Research*  
662 *Letters*, 43(20).
- 663 Davis, G.A., Cong, W., Yadong, Z., Jinjiang, Z., Changhou, Z., Gehrels, G.E., 1998. The  
664 enigmatic Yinshan fold-and-thrust belt of northern China: new views on its intraplate  
665 contractional styles. *Geology* 26, 43–46.
- 666 Ducassou E., Mulder T., Migeon S., et al., 2008. Nile floods recorded in deep Mediterranean

- 667 sediments. Quat. Res., 70, 382–391.
- 668 Dumont, H. J. and Negrea, S. V. 2002. *Introduction to the class Branchiopoda*. Leiden:
- 669 Backhuys.
- 670 Duncan, I.J., Titchener, F., Briggs, D.E.G., 2003. Decay and disarticulation of the cockroach:
- 671 implications for preservation of the blattoids of Writhlington (Upper Carboniferous), UK.
- 672 Palaios 18, 256–265.
- 673 Fisher, R.V., Schmincke, H.–U., 2012. Pyroclastic rocks. Springer Science & Business
- 674 Media.
- 675 Frank, P., 1988. Conchostraca. Palaeogeogr. Palaeoclimatol. Palaeoecol. 62, 399–403.
- 676 Gao, K.-Q., Chen, J., Jia, J., 2013. Taxonomic diversity, stratigraphic range, and exceptional
- 677 preservation of Juro–Cretaceous salamanders from northern China. Can. J. Earth Sci. 50,
- 678 255–267.
- 679 Gao, K.-Q., Shubin, N.H., 2003. Earliest known crown-group salamanders. Nature 422, 424–
- 680 428.
- 681 He, H. Y., Wang, X. L., Zhou, Z. H., Zhu, R. X., Jin, F., Wang, F., Ding, X., Boven, A., 2004.
- 682  $^{40}\text{Ar}/^{39}\text{Ar}$  dating of ignimbrite from Inner Mongolia, northeastern China, indicates a post-
- 683 Middle Jurassic age for the overlying Daohugou Bed. Geophys. Res. Lett., 31, 1–4.
- 684 Heiken, G., 1972. Morphology and petrography of volcanic ashes. Geol. Soc. Am. Bull. 83,
- 685 1961–1988.
- 686 Hethke, M., Fürsich, F.T., Jiang, B., Wang, B., Chellouche, P., Weeks, S.C. submitted.
- 687 Ecological stasis in Spinicaudata (Crustacea: Branchiopoda)? – Early Cretaceous clam
- 688 shrimp of the Yixian Formation of NE China occupied a broader realized ecological niche



- 689 than extant members of the group.
- 690 Horton, B.K., Schmitt, J.G., 1996. Sedimentology of a lacustrine fan-delta system, Miocene  
691 Horse Camp Formation, Nevada, USA. *Sedimentology* 43, 133–155.
- 692 Huang, D., 2015. Yanliao biota and Yanshan movement. *Acta Palaeontol. Sin.* 54, 501–546.
- 693 Huang, D.Y. (Ed.), 2016. The Daohugou Biota. Shanghai Science and Technical Publishers,  
694 Shanghai, 332 pp.
- 695 Huang, D., Engel, M.S., Cai, C., Wu, H., Nel, A., 2012. Diverse transitional giant fleas from  
696 the Mesozoic era of China. *Nature* 483, 201–204.
- 697 Huang, D., Nel, A., Shen, Y., Selden, P., Lin, Q., 2006. Discussions on the age of the  
698 Daohugou fauna-evidence from invertebrates. *Progr. Nat. Sci.* 16, 309–312.
- 699 Huang, D.Y., Cai, C.Y., Jiang, J.Q., Yi-Tong, S.U., Liao, H.Y., 2015. Daohugou bed and  
700 fossil record of its basal conglomerate section. *Acta Palaeontol. Sin.* 54, 501–546.
- 701 Hudspith, V.A., Scott, A.C., Wilson, C.J., Collinson, M.E., 2010. Charring of woods by  
702 volcanic processes: an example from the Taupo ignimbrite, New Zealand. *Palaeogeogr.*  
703 *Palaeoclimatol. Palaeoecol.* 291, 40–51.
- 704 Huff, W. D., 2016. K-bentonites: A review. *Am. Mineral.* 101, 43–70.
- 705 Hungr, O., Evans, S., Bovis, M., Hutchinson, J., 2001. A review of the classification of  
706 landslides of the flow type. *Environ. Eng. Geosci.* 7, 221–238.
- 707 Jansson, A., & Reavell, P. E., 1999. North American species of *Trichocorixa* (Heteroptera:  
708 *Corixidae*) introduced into Africa. *Afr. Entomol.* 7, 295–297.
- 709 Ji, Q., Luo, Z.-X., Yuan, C.-X., Tabrum, A.R., 2006. A swimming mammaliaform from the  
710 Middle Jurassic and ecomorphological diversification of early mammals. *Science* 311,

- 711 1123–1127.
- 712 Jiang, B., 2006. Non-marine Ferganoconcha (Bivalvia) from the Middle Jurassic in Daohugou  
713 area, Ningcheng County, Inner Mongolia, China. *Acta Palaeontol. Sin.* 45, 252–257.
- 714 Jiang, B.Y., Harlow, G.E., Wohletz, K., Zhou, Z., Meng, J., 2014. New evidence suggests  
715 pyroclastic flows are responsible for the remarkable preservation of the Jehol biota. *Nat.*  
716 *Commun.* 5, 3151. <http://dx.doi.org/10.1038/ncomms4151>.
- 717 Jiang, B., Sha, J., 2006. Late Mesozoic stratigraphy in western Liaoning, China: a review. *J.*  
718 *Asian Earth Sci.* 28, 205–217.
- 719 Kassem, A., Imran, J., 2001. Simulation of turbid underflows generated by the plunging of a  
720 river. *Geology* 29, 655–658.
- 721 Kellner, A.W., Wang, X., Tischlinger, H., de Almeida Campos, D., Hone, D.W., Meng, X.,  
722 2010. The soft tissue of *Jeholopterus* (Pterosauria, Anurognathidae, Batrachognathinae)  
723 and the structure of the pterosaur wing membrane. *Proc. R. Soc. Lond. B: Biol. Sci.* 277,  
724 321–329.
- 725 Kidwell, S.M., Fuersich, F.T., Aigner, T., 1986. Conceptual framework for the analysis and  
726 classification of fossil concentrations. *Palaios* 1, 228–238.
- 727 Larsen, D., Crossey, L.J., 1996. Depositional environments and paleolimnology of an ancient  
728 caldera lake: Oligocene Creede Formation, Colorado. *Geol. Soc. Am. Bull.* 108, 526–544.
- 729 Li, Q., Clarke, J. A., Gao, K. Q., Zhou, C. F., Meng, Q., Li, D., et al., 2014. Melanosome  
730 evolution indicates a key physiological shift within feathered dinosaurs. *Nature*, 507, 350-  
731 353.
- 732 Li, S., Wang, J., Wang, X., 1996. Stratigraphy (lithostratic) of Hebei Province. China

- University of Geosciences Press, Wuhan, pp. 60–73.
- Liao, H. Y., Shen, Y. B., Huang, D. Y., 2017. Conchostracans of the Middle–Late Jurassic Daohugou and Linglongta beds in NE China. *Palaeoworld*, 26, 317–330.
- Liu, P., Huang, J., Ren, D., 2010. Palaeoecology of the Middle Jurassic Yanliao entomofauna. *Acta Zootaxon. Sin.* 35, 568–584.
- Liu, Y., Liu, Y., Zhang, H., 2006. LA-ICPMS Zircon U-Pb Dating in the Jurassic Daohugou Beds and Correlative Strata in Ningcheng of Inner Mongolia. *Acta Geol. Sin. (English Edition)*, 80, 733–742.
- Liu, Y., Liu, Y., Li, P., Zhang, H., Zhang, L., Li, Y., Xia, H., 2004. Daohugou biota-bearing lithostratigraphic succession on the southeastern margin of the Ningcheng basin, Inner Mongolia, and its geochronology. *Region. Geol. Chin.* 23, 1180–1187.
- Lofgren G. Experimentally produced devitrification textures in natural rhyolitic glass. *Geol. Soc. Am. Bull.* 82, 111–124.
- Lü, J., Unwin, D.M., Jin, X., Liu, Y., Ji, Q., 2010. Evidence for modular evolution in a long-tailed pterosaur with a pterodactyloid skull. *Proc. R. Soc. Lond. B: Biol. Sci.* 277, 383–389.
- Luo, Z.-X., Ji, Q., Yuan, C.-X., 2007. Convergent dental adaptations in pseudo-tribosphenic and tribosphenic mammals. *Nature* 450, 93–97.
- Luo, Z.-X., Meng, Q.-J., Ji, Q., Liu, D., Zhang, Y.-G., Neander, A.I., 2015. Evolutionary development in basal mammaliaforms as revealed by a docodontan. *Science* 347, 760–764.
- Luo, Z.-X., Yuan, C.-X., Meng, Q.-J., Ji, Q., 2011. A Jurassic eutherian mammal and divergence of marsupials and placentals. *Nature* 476, 442.

- 
- 755 Lyman, F. E., 1943. Swimming and burrowing activities of mayfly nymphs of the genus  
756 *Hexagenia*. Ann. Entomol. Soc. Am. 36, 250–256.
- 757 Mandeville, C.W., Carey, S., Sigurdsson, H., 1996. Sedimentology of the Krakatau 1883  
758 submarine pyroclastic deposits. Bull. Volcanol. 57, 512–529.
- 759 Manville, V., Németh, K., Kano, K., 2009. Source to sink: a review of three decades of  
760 progress in the understanding of volcanoclastic processes, deposits, and hazards. Sediment.  
761 Geol. 220, 136–161.
- 762 Manville, V., White, J. D. L., Riggs, N. R., 2001. Sedimentology and history of Lake  
763 Reporoa: an ephemeral supra-ignimbrite lake, Taupo Volcanic Zone, New Zealand.  
764 Volcanoclastic Sedimentation in Lacustrine Settings, Int. Ass. Sedimentol. Spec. Publ. 30,  
765 109–140.
- 766 Martínez-Delclòs, X., Martinell, J., 1993. Insect taphonomy experiments. Their application to  
767 the Cretaceous outcrops of lithographic limestones from Spain. Kaupia 2, 133–144.
- 768 Martin, T., Marugán-Lobón, J., Vullo, R., Martín-Abad, H., Luo, Z.-X., Buscalioni, A.D.,  
769 2015. A Cretaceous eutriconodont and integument evolution in early mammals. Nature  
770 526, 380–384.
- 771 McPhie, J., 1986. Primary and redeposited facies from a large-magnitude, rhyolitic,  
772 phreatomagmatic eruption: Cana Creek Tuff, Late Carboniferous, Australia. J. Volcanol.  
773 Geotherm. Res. 28, 319–350.
- 774 Meng, J., Hu, Y., Wang, Y., Wang, X., Li, C., 2006. A Mesozoic gliding mammal from  
775 northeastern China. Nature 444, 889–893.
- 776 Meng, Q.-R., 2003. What drove late Mesozoic extension of the northern China-Mongolia

- 777 tract? *Tectonophysics* 369, 155–174.
- 778 Mulder, T., Alexander, J., 2001. The physical character of subaqueous sedimentary density  
779 flows and their deposits. *Sedimentology* 48, 269–299.
- 780 Mulder, T., Chapron, E., 2011. Flood deposits in continental and marine environments:  
781 character and significance. In: Slatt, R.M., Zavala, C (Eds.), *Sediment Transfer from Shelf  
782 to Deep Water – Revisiting the Delivery System*, AAPG Studies in Geology, 61, pp. 1–30.
- 783 Na, Y., Manchester, S.R., Sun, C., Zhang, S., 2015. The Middle Jurassic palynology of the  
784 Daohugou area, Inner Mongolia, China, and its implications for palaeobiology and  
785 palaeogeography. *Palynology* 39, 270–287.
- 786 Na, Y., Sun, C., Wang, H., Dilcher, D.L., Li, Y., 2017. A brief introduction to the Middle  
787 Jurassic Daohugou Flora from Inner Mongolia. *Rev. Palaeobot. Palynol.* 247, 53–67.
- 788 Nelson, C.H., Meyer, A.W., Thor, D., Larsen, M., 1986. Crater Lake, Oregon: A restricted  
789 basin with base-of-slope aprons of nonchannelized turbidites. *Geology* 14, 238–241.
- 790 Nemec, W., Steel, R., 1988. What is a fan delta and how do we recognize it? In: Nemec, W.,  
791 Steel, R. (Eds.), *Fan Deltas: sedimentology and tectonic settings*. Blackie & Son,  
792 Edinburgh, pp. 3–13.
- 793 Nie, S., Rowley, D., Ziegler, A., 1990. Constraints on the locations of Asian microcontinents  
794 in Palaeo-Tethys during the Late Palaeozoic. *Geol. Soc. Lond. Mem.* 12, 397–409.
- 795 Niem, A.R., 1977. Mississippian pyroclastic flow and ash-fall deposits in the deep-marine  
796 Ouachita flysch basin, Oklahoma and Arkansas. *Geol. Soc. Am. Bull.* 88, 49–61.
- 797 Olempska, E., 2004. Late Triassic spinicaudatan crustaceans from southwestern Poland. *Acta  
798 Palaeontol. Pol.* 49, 429–442.

- 
- 799 Olsen, P. E. 2016. The paradox of “clam shrimp” paleoecology. International Geological  
800 Congress, Abstracts, v. 35; 35th international geological congress, Cape Town, South  
801 Africa, Aug. 27-Sept. 4, 2016.
- 802 Palmer, B. A., & Shawkey, E. P., 1997. Lacustrine sedimentation processes and patterns  
803 during effusive and explosive volcanism, Challis volcanic field, Idaho. *J. Sediment. Res.*  
804 67, 154–167.
- 805 Palmer, B. A., & Shawkey, E. P., 2001. Lacustrine-fluvial transitions in a small intermontane  
806 valley, Eocene Challis Volcanic Field, Idaho. In: White, J.D.L., Riggs, N.R. (Eds.),  
807 Volcaniclastic Sedimentation in Lacustrine Settings. International Association of  
808 Sedimentologists, Special Publication 30, 179–198.
- 809 Parsons, J. D., Bush, J. W., Syvitski, J. P., 2001. Hyperpycnal plume formation from riverine  
810 outflows with small sediment concentrations. *Sedimentology*, 48, 465–478.
- 811 Pott, C., Jiang, B., 2017. Plant remains from the Middle–Late Jurassic Daohugou site of the  
812 Yanliao Biota in Inner Mongolia, China. *Acta Palaeobot.* 57, 185–222.
- 813 Pozzuoli, A., Vila, E., Franco, E., Ruiz–Amil, A., & De La Calle, C., 1992. Weathering of  
814 biotite to vermiculite in Quaternary lahars from Monti Ernici, central Italy. *Clay Minerals*  
815 27, 175–184.
- 816 Reineck, H.-E., Singh, I.B., 2012. Depositional sedimentary environments: with reference to  
817 terrigenous clastics. Springer Science & Business Media.
- 818 Ren, D., Gao, K., Guo, Z., Ji, S., Tan, J., Song, Z., 2002. Stratigraphic division of the Jurassic  
819 in the Daohugou area, Ningcheng, Inner Mongolia. *Geol. Bull. Chin.* 21, 584–591.
- 820 Riggs, N.R., Busby-Spera, C.J., 1990. Evolution of a multi-vent volcanic complex within a

- 
- 821 subsiding arc graben depression: Mount Wrightson Formation, Arizona. *Geol. Soc. Am.*  
822 *Bull.* 102, 1114–1135.
- 823 Schmid, R., 1981. Descriptive nomenclature and classification of pyroclastic deposits and  
824 fragments: Recommendations of the IUGS Subcommittee on the Systematics of Igneous  
825 Rocks. *Geology* 9, 41–43.
- 826 Scott, W. E., Hoblitt, R. P., Torres, R. C., Self, S., Martinez, M. M. L., Nillos, T., 1996.  
827 Pyroclastic flows of the June 15, 1991, climactic eruption of Mount Pinatubo. *Fire and*  
828 *Mud: eruptions and lahars of Mount Pinatubo, Philippines*, 545–570.
- 829 Self, S., 1983. Large-scale phreatomagmatic silicic volcanism: a case study from New  
830 Zealand. *J. Volcanol. Geotherm. Res.* 17, 433–469.
- 831 Shen, Y., Chen, P., Huang, D., 2003. Age of the fossil conchostracans from Daohugou of  
832 Ningcheng, Inner Mongolia. *J. Stratigr.* 27, 311–313.
- 833 Sheridan, M.F., Wohletz, K.H., 1981. Hydrovolcanic explosions: the systematics of water-  
834 pyroclast equilibration. *Science* 212, 1387–1389.
- 835 Sigurdsson, H., Cashdollar, S., Sparks, S.R.J., 1982. The eruption of Vesuvius in A.D. 79:  
836 reconstruction from historical and volcanological evidence. *Am. J. Archaeol.* 86, 39–51.
- 837 Simon, A., 1999. Channel and drainage-basin response of the Toutle River system in the  
838 aftermath of the 1980 eruption of Mount St. Helens, Washington, U.S. Geological Survey  
839 Open-File Report, 96-633. 130 pp.
- 840 Smith, G.A., 1988. Sedimentology of proximal to distal volcanoclastics dispersed across an  
841 active foldbelt: Ellensburg Formation (late Miocene), central Washington. *Sedimentology*  
842 35, 953–977.



- 843 Smith, G.A., 1991. Facies sequences and geometries in continental volcanoclastic sediments.  
844 In: Fisher, R.V., Smith, G.A. (Eds.), *Sedimentation in Volcanic Settings*: Soc. Econ.  
845 Paleontol. Mineral. Spec. Publ. 45, 10–25. Tulsa, Ok.
- 846 Smith, R., 1986. Sedimentation and palaeoenvironments of Late Cretaceous crater-lake  
847 deposits in Bushmanland, South Africa. *Sedimentology* 33, 369–386.
- 848 Streck, M.J., Grunder, A.L., 1995. Crystallization and welding variations in a widespread  
849 ignimbrite sheet; the Rattlesnake Tuff, eastern Oregon, USA. *Bull. Volcanol.* 57, 151–169.
- 850 Sturm, M., 1979. Origin and composition of clastic varves. In: C. Schüchter (ed.), *Moraines*  
851 *and Varves*. Balkema, Rotterdam, pp. 281–285.
- 852 Sturm, M., Matter, A., 1978. Turbidites and varves in Lake Brienz (Switzerland): deposition  
853 of clastic detritus by density currents. In: Matter, A., Tucker, M.E. (Eds.), *Modern and*  
854 *Ancient Lake Sediments*. Spec. Publ. Int. Assoc. Sedimentol. 2, 147–168.
- 855 Sullivan, C., Wang, Y., Hone, D.W., Wang, Y., Xu, X., Zhang, F., 2014. The vertebrates of  
856 the Jurassic Daohugou Biota of northeastern China. *J. Vertebr. Paleontol.* 34, 243–280.
- 857 Tasch, P., 1969. Branchiopoda. RC Moore, ed. *Treatise on invertebrate paleontology*, part R,  
858 *Arthropoda* 4. Geol. Soc. Am. and Univ. Kans. Press, Lawrence.
- 859 Vannier, J., Thiery, A., Racheboeuf, P.R., 2003. Spinicaudatans and ostracods (Crustacea)  
860 from the Montceau Lagerstätte (Late Carboniferous, France): morphology and  
861 palaeoenvironmental significance. *Palaeontology* 46, 999–1030.
- 862 Wang, B., Li, J., Fang, Y., Zhang, H., 2009. Preliminary elemental analysis of fossil insects  
863 from the Middle Jurassic of Daohugou, Inner Mongolia and its taphonomic implications.  
864 *Chinese Sci. Bull.* 54, 783–787.

- 865 Wang, B., Zhang, H., Jarzembowski, E.A., Fang, Y., Zheng, D., 2013. Taphonomic  
866 variability of fossil insects: a biostratigraphic study of Palaeontinidae and Tettigarctidae  
867 (Insecta: Hemiptera) from the Jurassic Daohugou Lagerstätte. *Palaios* 28, 233–242.
- 868 Wang, W., Zheng, S., Zhang, L., Pu, R., Zhang, W., Wu, H., Ju, R., Dong, G., Yuan, H.,  
869 1989. Mesozoic stratigraphy and palaeontology of western Liaoning (1), Beijing: Geol.  
870 Pub. House (in Chinese with English abstract).
- 871 Wang, X., Wang, Y., Zhang, F., Zhang, J., Zhou, Z.-H., Jin, F., Hu, Y.-M., Gu, G., Hai-  
872 Chun, Z., 2000. Vertebrate biostratigraphy of the Lower Cretaceous Yixian Formation in  
873 Lingyuan, western Liaoning and its neighboring southern Nei Mongol (inner Mongolia),  
874 China. *Vertebr. Palasiat.* 38, 95–101.
- 875 Wang, X., Zhou, Z., He, H., Jin, F., Wang, Y., Zhang, J., Wang, Y., Xu, X., Zhang, F., 2005.  
876 Stratigraphy and age of the Daohugou bed in Ningcheng, Inner Mongolia. *Chinese Sci.*  
877 *Bull.* 50, 2369–2376.
- 878 Webb, J., 1979. A reappraisal of the palaeoecology of conchostracans (Crustacea:  
879 Branchiopoda). *Neues Jahrb. Geol. Paläontol., Abh.* 158, 259–275.
- 880 Whitham, A., 1989. The behaviour of subaerially produced pyroclastic flows in a subaqueous  
881 environment: evidence from the Roseau eruption, Dominica, West Indies. *Mar. Geol.* 86,  
882 27–40.
- 883 Wilson, C., Walker, G.P., 1985. The Taupo eruption, New Zealand I. General aspects. *Phil.*  
884 *Trans. R. Soc. Lond. A* 314, 199–228.
- 885 Xu, H., Liu, Y.-Q., Kuang, H.-W., Jiang, X.-J., Peng, N., 2012. U-Pb SHRIMP age for the  
886 Tuchengzi Formation, northern China, and its implications for biotic evolution during the

- 887 Jurassic–Cretaceous transition. *Palaeoworld* 21, 222–234.
- 888 Xu, X., You, H., Du, K., Han, F., 2011. An *Archaeopteryx*-like theropod from China and the  
889 origin of Avialae. *Nature* 475, 465–470.
- 890 Xu, X., Zhang, F., 2005. A new maniraptoran dinosaur from China with long feathers on the  
891 metatarsus. *Naturwissenschaften* 92, 173–177.
- 892 Xu, X., Zhao, Q., Norell, M., Sullivan, C., Hone, D., Erickson, G., Wang, X., Han, F., Guo,  
893 Y., 2009. A new feathered maniraptoran dinosaur fossil that fills a morphological gap in  
894 avian origin. *Chinese Sci. Bull.* 54, 430–435.
- 895 Xu, X., Zheng, X., Sullivan, C., Wang, X., Xing, L., Wang, Y., Zhang, X., O'Connor, J.K.,  
896 Zhang, F., Pan, Y., 2015. A bizarre Jurassic maniraptoran theropod with preserved  
897 evidence of membranous wings. *Nature* 521, 70–73.
- 898 Xu, X., Zhou, Z., Dudley, R., Mackem, S., Chuong, C.-M., Erickson, G.M., Varricchio, D.J.,  
899 2014. An integrative approach to understanding bird origins. *Science* 346, 1253293.
- 900 Xu, X., Zhou, Z., Sullivan, C., Wang, Y., Ren, D., 2016. An updated review of the  
901 Middle-Late Jurassic Yanliao Biota: chronology, taphonomy, paleontology and  
902 paleoecology. *Acta Geol. Sin. Engl.* 90, 2229–2243.
- 903 Yang, W., Li, S., 2008. Geochronology and geochemistry of the Mesozoic volcanic rocks in  
904 Western Liaoning: implications for lithospheric thinning of the North China Craton. *Lithos*  
905 102, 88–117.
- 906 Yang, X., Li, X., Sun, J., 1997. Stratigraphy (lithostratic) of Liaoning Province. Wuhan:  
907 China University of Geosciences Press.
- 908 Yin, A., Nie, S., 1996. A Phanerozoic palinspastic reconstruction of China and its neighboring

- 
- 909 regions. *World and Regional Geology* 1, 442–485.
- 910 Yuan, W., 2000. A new salamander (Amphibia: Caudata) from the Early Cretaceous Jehol  
911 biota. *Vertebr. Palasiat.* 2, 002.
- 912 Yuan, W., Liping, D., Evans, S.E., 2010. Jurassic–Cretaceous herpetofaunas from the Jehol  
913 associated strata in NE China: evolutionary and ecological implications. *Bull. Chinese*  
914 *Acad. Sci.* 24, 76–79.
- 915 Zhang, F., Zhou, Z., Xu, X., Wang, X., Sullivan, C., 2008. A bizarre Jurassic maniraptoran  
916 from China with elongate ribbon-like feathers. *Nature* 455, 1105–1108.
- 917 Zhang, J., 2002. Discovery of Daohugou Biota (Pre-Jehol Biota) with a discussion on its  
918 geological age. *J. Stratigr.* 26, 173–177.
- 919 Zhang, Y., Dong, S., Zhao, Y., Zhang, T., 2008. Jurassic tectonics of North China: a synthetic  
920 view. *Acta Geol. Sin. Engl.* 82, 310–326.
- 921 Zhou, Z.H., Jin, F., and Wang, Y., 2010. Vertebrate assemblages from the Middle-Late  
922 Jurassic Yanliao Biota in northeast China. *Earth Sci. Frontiers*, 17: 252–254.
- 923 Zhou, Z., Zheng, S., Zhang, L., 2007. Morphology and age of *Yimaia* (Ginkgoales) from  
924 Daohugou Village, Ningcheng, Inner Mongolia, China. *Cretaceous Res.* 28, 348–362.
- 925 Ziegler, A.M., Rees, P.M., Rowley, D.B., Bekker, A., Qing, L., Hulver, M.L., 1996. Mesozoic  
926 assembly of Asia: constraints from fossil floras, tectonics, and paleomagnetism. In: Yin,  
927 A., Harrison, T.M. (Eds.), *Tectonic evolution of Asia*. Cambridge Univ. Press, Cambridge,  
928 pp. 371–400.

## 1 Appendix 1. Supplementary methods

### 2 1. X-ray diffraction analysis

3 Two specimens of insect-bearing laminated mudstone were pulverized without  
4 cross contamination before XRD analysis. The prepared samples were then analyzed  
5 for mineralogy by XRD using Rigaku, Ultima IV with D/teX Ultra, at the Institute of  
6 Soil Science, Chinese Academy of Science.

7

### 8 2. Plan-view orientation measurement

9 Plan-view orientations of the aquatic insects *Fuyous gregarious*, *Shantous*  
10 *lacustris*, and *Daohugocorixa vulcanica* were obtained from nine horizons (A1, B1, B2,  
11 C1, E2, F1, I1, I3, I4, Fig. 2A) by subdividing a circle into 12 segments and counting  
12 the orientation of each individual. Two individuals whose heads point in opposite  
13 directions are treated as showing the same orientation. Hence, the segments 7–12 were  
14 mirrored, and only six directions (0–180°) remained to test for preferred orientations  
15 using Rayleigh's test and the Chi-square test (Hethke et al., submitted). Rayleigh's test  
16 is based on data drawn from a population with a von Mises distribution (Davis, 1986).  
17 Rayleigh's test has the following null and alternative hypotheses:

18  $H_0$ : the directions of aquatic insects are uniformly distributed

19  $H_1$ : there is a single preferred direction

20 Similarly, the null and alternative hypotheses of Chi-square test are:

21  $H_0$ : the directions of aquatic insects are uniformly distributed

22  $H_1$ : the directions of aquatic insects are not uniformly distributed

23 These two tests are used together to test for preferred orientations using the scheme

24 of Hammer and Harper (2006).

25

26   **References**

27    Davis, J., 1986, Statistics and Data Analysis in Geology, John Wiley &amp; Sons Canada,

28       Ltd.

29    Hammer, Ø., Harper, D., 2006 Paleontological data analysis. – Blackwell Publishing.

30    Hethke, M., Fürsich, F.T., Jiang, B., Wang, B., Chellouche, P., Weeks, S.C. submitted.

31       Ecological stasis in Spinicaudata (Crustacea: Branchiopoda)? – Early Cretaceous

32       clam shrimp of the Yixian Formation of NE China occupied a broader realized

33       ecological niche than extant members of the group. Palaeontology.

34

35



## Appendix 2. Supplementary results

### 1. X-ray diffraction (XRD) analysis

	Montmorillonite	Vermiculite	Illite	Aluminite	Quartz	Feldspar	Dolomite
Sample 1	24%	26%	22%	0%	14%	12%	2%
Sample 2	19%	19%	11%	14%	17%	19%	1%
Mean	21.5%	22.5%	16.5%	7%	15.5%	15.5%	1.5%

**Table 1** XRD analysis of the fossil-bearing mudstone from Unit 3.

39

### 2. Plan-view orientation

Horizons	n	Mean	R	P (Rand)	Chi <sup>2</sup>	P (Rand)
A1	16	83.05	0.2253	0.45	6.5	0.26
B1	16	96.95	0.2253	0.45	5	0.42
B2	77	27.64	0.1368	0.24	39.96	1.52E-07
C1	103	68.74	0.112	0.28	33.49	3.01E-06
E2	13	45	0.2665	0.41	8.69	0.122
F1	27	83.05	0.1335	0.62	16.33	0.006
I1	17	60	0.3529	0.12	6.65	0.25
I3	110	86.39	0.1879	0.02	26.58	6.88E-05
I4	24	80.45	0.1102	0.75	10	0.075

**Table 2** Test results (Rayleigh and Chi-square) based on directional measurements of aquatic insects in nine horizons (locations shown in Fig. 2A).

43

44       Based on the results of the Chi-square test, aquatic insects of horizons B2, C1,  
45   F1 and I3 exhibit preferred orientations. The null hypothesis of random orientation  
46   can be rejected at a significance level of 1%. Among these four horizons, Rayleigh's  
47   test further indicates a single preferred orientation in I3 at 5% significance level,  
48   while the null hypothesis could not be rejected for B2, C1, and F1, implying two or  
49   more preferred orientations in the respective horizons (Appendix 2, Table 2).